Effects of Different Doses of Calcium on the Mitochondrial Apoptotic Pathway and Rho/ROCK Signaling Pathway in the Bone of Fluorosis Rats

Jiarong Yang[1,2] · Yaya Zhu[1,2] · Dongfang Zhang[2] · Zipeng Yan[1,2] · Yangfei Zhao[1,2] · Ram Kumar Manthari[1,2] · Xiaofang Cheng[3] · Jundong Wang[1,2] · Jinming Wang[1,2]

Abstract

For this study, we investigate more deeply the effect calcium (Ca) develops on the mechanism underlying fluoride-triggered osteocyte apoptosis. We detected the morphology of osteocytes by HE staining, mitochondrial microstructure by using the transmission electron microscope, and the biochemical indexes related to bone metabolism and the expression of apoptosis-related genes. These results showed that NaF brought out the reduced osteocytes and ruptured mitochondrial outer membrane, with a significantly increased StrACP activity by 10.414 IU/L at the 4th week ($P < 0.05$), markedly upregulating the mRNA expression of Bax, Cyto-C, Apaf-1, caspase-7, ROCK-1, BMP-2, and BGP ($P < 0.01$), as well as caspase-6 ($P < 0.05$), while downregulating Bcl-2 by 61.3% ($P < 0.01$). Through immunohistochemical analysis, we also found that NaF notably increased the protein expression of ROCK-1 ($P < 0.05$) and Cyto-C, BMP-2, and BGP ($P < 0.01$), suggesting that NaF triggered the activation of the mitochondrial apoptotic pathway and Rho/ROCK signaling pathway. Nevertheless, 1% Ca supplementation in diet notably enhanced the mRNA expression of Bcl-2 by 39.3% ($P < 0.01$), thus blocking the increment of the expression of mitochondrial apoptotic pathway–related genes and ROCK-1. Meanwhile, Ca could attenuate the StrACP activity by 10.741 IU/L at the 4th week ($P < 0.05$) and protect the integrity of the mitochondrial outer membrane. These findings strongly suggest that 1% Ca abated the mitochondrial apoptosis pathway by increasing the anti-apoptotic gene Bcl-2 expression, and effectively inhibited the hyper-activation of ROCK-1, dually protecting the structural integrity of the mitochondrial outer membrane and maintaining normal cellular metabolic function.

Keywords Apoptosis · Bone injury · Calcium · Fluorosis · Mitochondria

Introduction

Fluorosis is a common endemic disease in humans and animals worldwide, and its clinical features are dental fluorosis and skeletal fluorosis [1]. The effects of fluoride (F) on bone health are mainly reflected in bone mass and its metabolism.

The comprehensive studies that explored the mechanisms underlying skeletal fluorosis indicated that enhanced osteogenic and osteoclastogenic activities were mediated by many proteins and enzymes associated with bone metabolism [2, 3]. Osteoblasts (OB), the main functional cells, regulate and influence the process of bone formation and reconstruction in bone formation [4]. OB are mainly derived from the differentiation of the inner and outer periosteum and mesenchymal progenitor cells in the bone marrow, which can specifically secrete a variety of bioactive substances including alkaline phosphatase (AKP), an indicator of bone turnover and bone formation [5]. A total of 50% of serum AKP comes from the bone. In our previous study, it showed that the proliferation and differentiation of primary OB were triggered by 10^{-6} mol/L sodium fluoride (NaF) significantly; however, the higher dose of NaF showed the inhibitory effect on OB proliferation [6]. Also, other studies indicated that the apoptosis rate of OB isolated from skullcap was significantly increased at 22.1 mg/L NaF [7].

✉ Jinming Wang
jmwang@sxau.edu.cn

1 College of Veterinary Medicine, Shanxi Key Laboratory of Environmental Veterinary Medicine, Shanxi Agricultural University, Taigu, Jinzhong 030801, Shanxi, People's Republic of China

2 Shanxi Key Laboratory of Environmental Veterinary Medicine, Shanxi Agricultural University, Taigu, Jinzhong 030801, Shanxi, People's Republic of China

3 College of Arts and Sciences, Shanxi Agricultural University, Taigu, Jinzhong 030801, Shanxi, People's Republic of China

As the functional cells in bone resorption, osteoclasts (OC) play a vital role in skeletal growth, development, repair, and reconstruction [8]. Tartrate-resistant acid phosphatase (StrACP), the dominant enzyme secreted by OC during bone resorption, is a sensitive index of bone resorption [9]. Also, studies have shown that skeletal fluorosis is accompanied by abnormalities in bone calcium (Ca) and phosphorus metabolism as well as hypocalcemia, increased bone turnover, and bone reconstruction [10, 11]. Bone morphogenetic protein-2 (BMP-2), a member of the bone morphogenetic proteins (BMPs), can induce undifferentiated mesenchymal stem cells to differentiate and proliferate into chondroblasts and OB. It also contributes to the growth and development of bone and cartilage and its regeneration process by promoting OB differentiation and maturation [12]. Bone gamma-carboxyglutamate protein (BGP) is synthesized by OB during bone matrix mineralization. The study found that the production of BGP increased with the progression of mineralization and OB differentiation [13]. The high NaF condition can lead to OB apoptosis and reduced activity, resulting in disordered matrix calcification and collagen synthesis, which ultimately severely reduces bone mass [14].

The changes in bone tissue metabolism are related not only to the damage of bone cell structure but also to the molecular mechanism of apoptosis. The mitochondrial apoptotic pathway has been proved to be one of the main pathways of apoptosis [15]. After the cells are stimulated by the death signal, B cell lymphoma 2 (Bcl-2)–associated X protein (Bax) is transferred from the cytoplasm to the mitochondrial outer membrane, destroying mitochondrial integrity and altering its permeability [16]. Cytochrome C (Cyto-C) is physiologically located in the intima of the mitochondria. Underlying factors such as Ca overload, hypoxia, ischemia, and reactive oxygen species could change the mitochondrial permeability and the release of Cyto-C [17]. Cyto-C released in the cytoplasm binds to apoptotic protease–activating factor-1 (Apaf-1) and aggregates with procaspase-9, leading to the decomposition of procaspase-9 and activation of caspase-9, resulting to the activation of caspase-6 and caspase-7 [18]. As an anti-apoptotic effector, a large number of studies have shown that Bcl-2 in the cytoplasm forms heterodimers with Bax released by mitochondria, thereby preventing the apoptotic effect of Bax and protecting mitochondrial integrity [19].

What is more, it has been verified that Rho-associated coiled coil–forming protein kinase (ROCK-1 and ROCK-2) participates in smooth muscle contraction and apoptosis [20]. Meanwhile, the Rho/ROCK pathway is a crucial component of axon-guided cell contraction and apoptosis regulation [21]. However, the exact role of the Rho/ROCK pathway in osteocyte apoptosis induced by F remains unclear. Furthermore, the role and mechanism of Ca in the apoptosis of bone through the Rho/ROCK pathway and mitochondrial apoptosis pathway mediated by Cyto-C/Apaf-1 have not been fully elucidated.

It has been proved that Ca inhibits F absorption in the gastrointestinal tract by forming insoluble CaF_2 deposition in the blood [22]. F affects Ca absorption, resulting in low blood Ca and bone salt dissolution, which is the pathological basis of loose and softened bone mass; hence, Ca supplementation is considered to be an effective drug for the treatment of fluorosis.

Therefore, we explored the role of Ca in apoptosis due to mitochondrial structure damage in F-induced osteoporosis and its effects on the mitochondrial apoptosis pathway through the Cyto-C/Apaf-1 and Rho/ROCK signaling pathways in the femora. Our findings might provide experimental and hypothetical guidance for subsequent studies of diseases associated with fluorosis.

Materials and Methods

Animals and Treatments

One hundred sixty healthy male rats 28 days old (weighed 120 ± 5 g), as well as rat standard pellet feed and standard powder feed, were obtained from the Shanxi Medical University Experimental Animal Center (Taiyuan, China). After 1-week acclimation, they were randomly designed into control (C), NaF (F), F+CaI, F+CaII, and F+CaIII groups (32 rats each group). The C group was fed with distilled water and basal pellet diet, and the F groups were given basal pellet food and distilled water containing 150 mg/L NaF. However, F+Ca groups were fed with distilled water containing 150 mg/L NaF and basal powder diet added with 0.5%, 1%, and 2% of $CaCO_3$ (Solarbio, Beijing, China) respectively. The rats were kept in standard cage with temperature around 20 ± 5 °C, 12-h light/dark cycle, and 40–60% humidity, and water and food pellets were freely available in their cages at all time.

After the 4th, 8th, 12th, and 16th weeks, 8 rats in each group were randomly selected for weighing and were killed by collecting blood from eyeballs after anesthesia. The whole blood was stratified at room temperature, centrifuged for 10 min with 3500 rpm/min to get the serum, and then stored in a − 80 °C refrigerator. The femora were collected at the 16th week. Some of the bone samples were fixed in 10% neutral buffer formalin solution for pathological section, while others were quick-frozen in liquid nitrogen and stored in a − 80 °C environment.

HE Staining to Detect the Effect of Different Ca Levels on Osteocytes

The femora were fixed in a 10% neutral formalin fixative for 24 h and then rinsed for 12 to 24 h, then immersed in ethylene diamine tetraacetic acid (EDTA) decalcified solution. Decalcified femora were cut into blocks horizontally to

Table 1 Primer sequences and corresponding PCR product size

No.	Gene	Primers (5′ > 3′)	Product Size (bp)	GenBank No.
1	Bax	GGATGGCCTCCTTTCCTACT AGCCTCAGCCCATCTTCTTC	110	NM-017059.2
2	Bcl-2	ATGATAACCGGGAGATCGTG CAGGCTGGAAGGAG AAGATG	135	NM-016993.1
3	Cyto-C	GGAGAGGATACCCTGATGGA GTCTGCCCTTTCTCCCTTCT	102	NM-012839.2
4	Apaf-1	AGAAGCTGGTCAGTGCGATT ACCTTCTAGGAGGGCATGGT	140	NM-023979.1
5	Caspase-6	AAGTGTCAGAGCCTGGTTGG TCGTCCAGCTTGTCTGTCTG	122	NM-001271984.1
6	Caspase-7	TTGGTGATGACAGGAATGGA ACTCCACTCAACAGCCACCT	129	NM-022260.3
7	ROCK-1	GTAATCGGCAGAGGTGCATT GCCATGATGTCCCTTTCTTC	146	NM-031098.1
8	BMP-2	CACGAGAATGGACGTGCCC GCAACACTAGAAGACAGCGG	96	NM-031098.1
9	BGP	TATGGCACCACCGTTTAGGG CCGTCCATACTTTCGAGGCA	118	NM_017178.1
10	β-actin	TGACAGGATGCAGA AGGAGA TAGAGCCACCAATCCACACA	104	NM_031144.3

prepare paraffin sections. Finally, the sections were stained by conventional HE staining, and the images were collected.

Transmission Electron Microscope

To observe the changes in the mitochondrial microstructure of femur, transmission electron microscopy (TEM) analysis was performed. The fresh femora were sawn into femoral plates and fixed in pre-cooling glutaraldehyde after saline rinse. Femur tablets were adequately rinsed in 0.2 mol/L phosphate buffer and then immersed in decalcification solution (4–5% EDTA-2Na) for 3 to 4 weeks. After 2 h of double fixation in 1% osmium tetroxide at 4 °C, the bone pieces were dehydrated step by step with 50%, 70%, 80%, 95%, and 100% acetone respectively. Finally, bone fragments were embedded, sliced, stained, and observed under an electron microscope [23].

Serum Ca, AKP, and StrAcp Determination

The contents of serum Ca, AKP, and StrAcp at the 4th, 8th, 12th, and 16th weeks were determined according to the instructions of the kit (provided by Nanjing Institute of Bioengineering, China).

Quantitative Real-Time PCR

After grounding into powder by liquid nitrogen, total RNA was extracted from femur using the RNAiso Plus Kit (TaKaRa Company, Dalian, China). After the concentration of RNA was determined by a nucleic acid protein analyzer, 1% agarose electrophoresis was used to examine its integrity and purity. Then, all samples were diluted to 250 ng/μL. A total of 750 ng RNA and 5 × PrimeScript^{TM} RT Master Mix were used for the reverse transcription (RT) test. The experimental primers of rat Bax, Bcl-2, Cyto-C, caspase-6, caspase-7, Apaf-1, BGP, BMP-2, ROCK-1, and β-actin were designed by using the Primer 5.0 primer design software (synthesized by Beijing Orco Dingsheng Biotechnology Co., Ltd.), shown in Table 1. The total reaction system of quantitative real-time PCR was 20 μL, which was performed by using the Agilent Mx3000P quantitative PCR system (USA) and SYBR Premix Ex Taq TM II kit (TaKaRa, Dalian, China). The PCR reaction conditions were maintained as follows: denaturation at 95 °C for 30 s, and 45 cycles of amplification are performed at 95 °C for 5 s, 62 °C for 34 s, and 95 °C for 15 s, as well as 60 °C for 1 min and 95 °C for 15 s for solubility curve analysis. Under the same conditions, the internal reference gene β-actin and target genes were amplified separately in different tubes. According to the amplification efficiency of the standard

curve, the difference of amplification efficiency between the target gene and internal reference gene was less than 5%. The relative expression of each target gene was calculated by using the $2^{-\triangle\triangle CT}$ method.

Determination of BGP, BMP-2, Cyto-C, and ROCK-1 Protein Expressions

Protein expressions related to bone metabolism and mitochondrial pathway as well as Rho/ROCK signaling pathway–related protein expression were detected by using the immunohistochemical method. After slicing, it is necessary to incubate in 3% H_2O_2 for 15 min at room temperature. The slices were immersed in antigen-repair solution (0.01 mol/L citrate buffer) and heated in a 100 °C water bath, then blocked at room temperature with 5% BSA for 20 min. The sections were incubated in a wet box with BGP (1:100 dilutions), BMP-2 (1: 200 dilutions), Cyto-C (1: 400 dilutions), and ROCK-1 (1:400 dilutions) rabbit anti-rat primary antibodies (Bioss Biotechnology Co., Ltd., Beijing, China) overnight at 4 °C, and second antibody was added for 20-min incubation at 37 °C. Then, the samples were colored with DAB (Wuhan Boster Biological Technology., Ltd., Wuhan, China) at room temperature for 10–30 min. Under the same conditions, the observed tissues were collected, and the optical density was calculated by using the image analysis software Image-Pro Plus v. 5.0. The average optical density of each positive area of each slice was calculated.

Statistical Analysis

The results were expressed with mean value ± SD (mean ± SD). Eight replicate assays were made in each group. The Prism 6 software was used to analyze the variance of the data in each experimental group. Analysis of variance (ANOVA) followed by Tukey's test regarded $P < 0.05$ as the significant difference.

Result

Effects of Different Ca Levels on Osteocytes in Fluorosis Rats

Osteocytes are visible and have uniform cell density in the C group (Fig. 1 a1). However, the osteocytes were reduced in number with malformation and unevenly distributed in the F group (Fig. 1 b1). The morphology of osteocytes was remarkably recovered and evenly distributed in the F+Ca groups (Fig. 1 c1–e1).
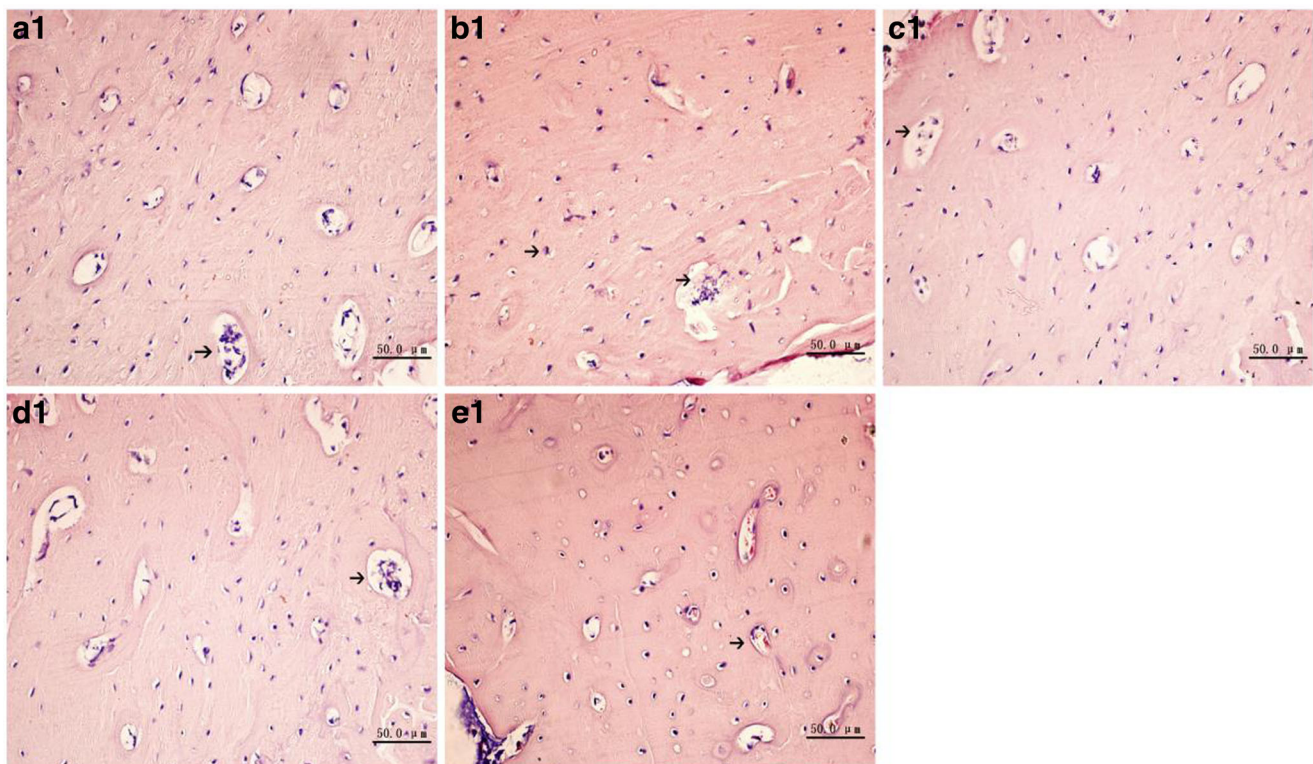
Fig. 1 a1–e1 Effects of Ca supplementation on osteocyte histopathology in rats. Arrows indicated the morphology of osteocytes; bar = 50 μm. a1 C group. b1 F group. c1 F+CaI group. d1 F+CaII group. e1 F+CaIII group
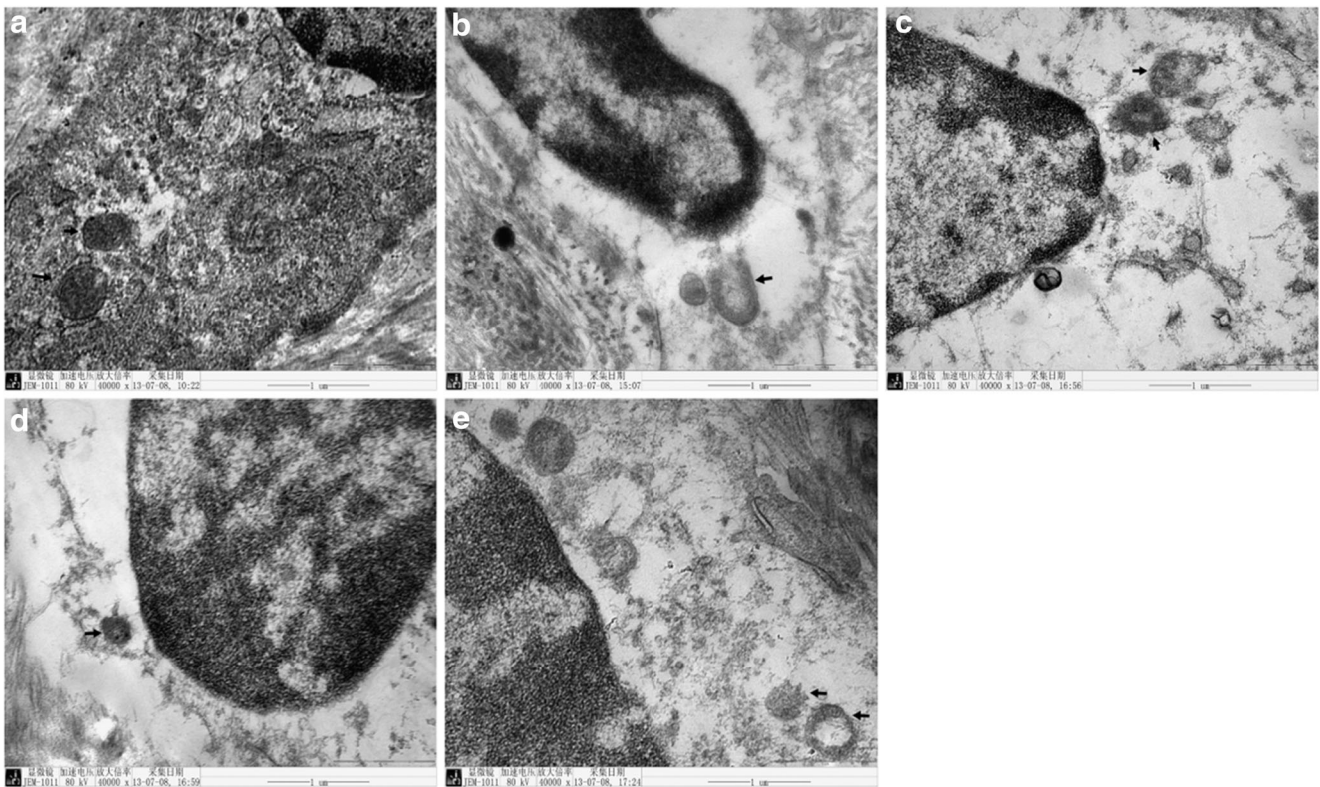
Fig. 2 **a**–**e** Effects of Ca supplementation on osteocyte mitochondrial ultrastructure in the osteocytes. Black arrows indicated the morphology of mitochondria; bar = 1 μm. The magnification of all the photograph is × 40,000. **a** C group. **b** F group. **c** F+CaI group. **d** F+CaII group. **e** F+CaIII group

Effects of Ca on Mitochondria Ultrastructure in the Osteocytes

The mitochondrial structure was normal, and the mitochondrial outer membrane was regarded as intact (Fig. 2a). The mitochondria in osteocytes were shown as cristae rupture, dissolution, and even vacuolization of mitochondria in the F group (Fig. 2b). The mitochondria of the F+CaII group were intact, and the membrane integrity was not destroyed (Fig. 2d). However, the mitochondria in the F+CaI group were characterized with swelling and mild cristae disorder (Fig. 2c), while the disappearance of crests and contents, as well as incomplete mitochondrial outer membrane, was observed in the F+CaIII group (Fig. 2e).

Effects of Different Ca Levels on Biochemical Indices Related to Bone Metabolism in Fluorosis Rats

In Fig. 3, the content of serum Ca (mmol/L) has shown a downward trend with no significance after F treatment. Nevertheless, the serum Ca level in the F+CaIII group was markedly upregulated at the 12th and 16th weeks ($P < 0.05$). AKP activity in the F group was higher than that in the C group, and F+Ca groups have less activity than those in the

F group, but there was no significant difference. The activity of StrACP in the F group was elevated ($P < 0.05$), whereas it was decreased markedly at the 4th week after 2% Ca supplementation diet ($P < 0.05$).

Effects of Different Ca Levels on the mRNA Expression of Osteocytes

The effect of Ca on bone metabolism and the mitochondrial pathway as well as Rho/ROCK signaling pathway–related mRNA are shown in Fig. 4. Compared with the C group, the mRNA expression levels of Bax, Cyto-C, Apaf-1, caspase-7, ROCK-1, BMP-2, and BGP ($P < 0.01$) as well as caspase-6 ($P < 0.05$) were obviously elevated. In contrast, the mRNA expression of Bcl-2 subjected to the F group was significantly less than that of normal rats, whereas it was improved with 1% and 2% Ca mitigation ($P < 0.01$). Compared with the F group, the enhanced mRNA expression of Bax, Cyto-C, Apaf-1, caspase-7, and ROCK-1 was attenuated by 0.5% Ca ($P < 0.01$), and Cyto-C, Apaf-1, and ROCK-1 ($P < 0.01$) as well as Bax, caspase-6, BMP-2, and BGP ($P < 0.05$) were markedly decreased by 1% and 2% Ca. Furthermore, the mRNA expression levels of Bax and ROCK-1 ($P < 0.01$), as well as Cyto-C and BGP ($P < 0.05$), were markedly downregulated with 2% Ca treatment.
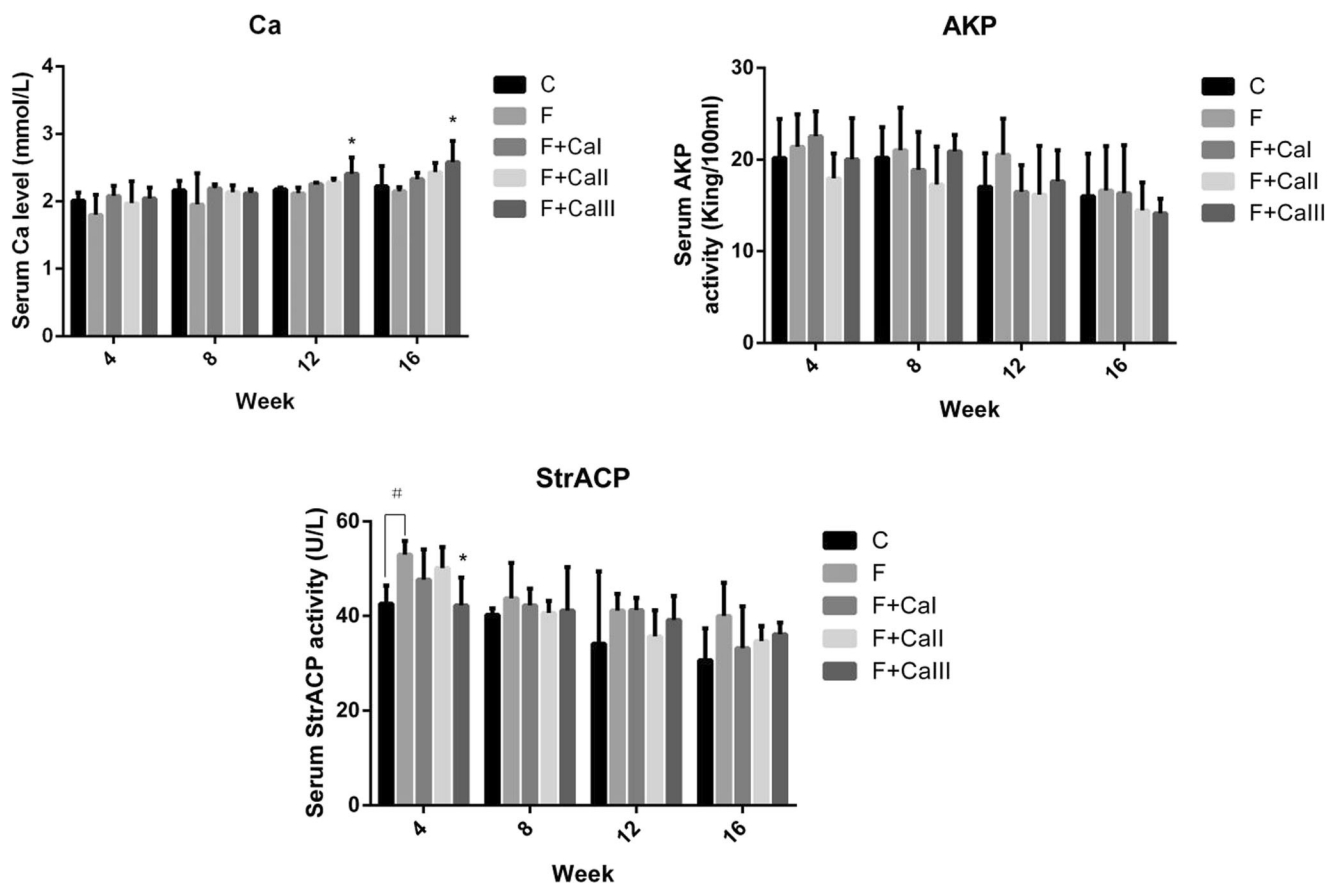
Fig. 3 Effects of different doses of Ca on bone metabolism–related indices at the 4th, 8th, 12th, and 16th weeks ($n = 8$). Serum Ca level, AKP activity, and serum StrACP activity in rats of each group with different exposure periods were depicted as mean ± SD ($n = 8$). [#]$P < 0.05$ as compared with the C group, [*]$P < 0.05$ as compared with the F group

Effects of Different Ca Levels on Bone Metabolism and Mitochondrial Pathway–Related Protein Expression in Osteocytes

As estimated by immunohistochemistry (Fig. 5), compared with the C group, the protein expression of ROCK-1 protein ($P < 0.05$), Cyto-C, BMP-2, and BGP ($P < 0.01$) was notably increased in the F group. In contrast, 1% Ca attenuated the enhanced protein expression of ROCK-1, BMP-2, and BGP induced by F ($P < 0.05$); 2% Ca blocked the elevated protein expression of Cyto-C and BGP triggered by F ($P < 0.01$, $P < 0.05$).

Discussion

F is a highly active natural halogen that is found in a variety of compounds, but excessive F intake is likely to damage organisms [24]. In our previous study, it was determined that F broaden the cortical thickness as well as the trabecular area of femur, and this result has also demonstrated that F caused the damage to osteocytes, and reduced the number and disrupted the arrangement of osteocytes in the femur [25].

Also, in our preliminary study, we found that the weight of the rats in the F group showed a downward trend, but the content of bone F⁻ increased significantly compared with the C group, which was shown in the previous studies [25].

Ca is the most important and abundant mineral element in the human body [26]. Studies have found that F and Ca have biological antagonism by forming insoluble CaF_2 sediments in the intestinal tract [22, 27]. In the current study, Ca supplementation reversed the F-induced osteocyte reduction, in line with our previous study [25].

Interestingly, through TEM analysis in this study, we found that the mitochondria of osteocytes in the femur were swollen, and the contents were missing with broken crests in the F group. A study has shown that NaF exposure increased cell apoptosis and the depolarization of the mitochondrial membrane potential (MMP) in ICR mice kidney [28]. Previous study has shown that the destruction of mitochondrial membrane structure may lead to the apoptosis in HeLa cells [29]. Therefore, it was hypothesized that disruption of mitochondrial membrane structure and dysfunction might be involved in the abnormal energy metabolism and apoptosis of osteocytes, thus leading to abnormal bone metabolization induced by 150 mg/L NaF exposure in this study, which was consistent
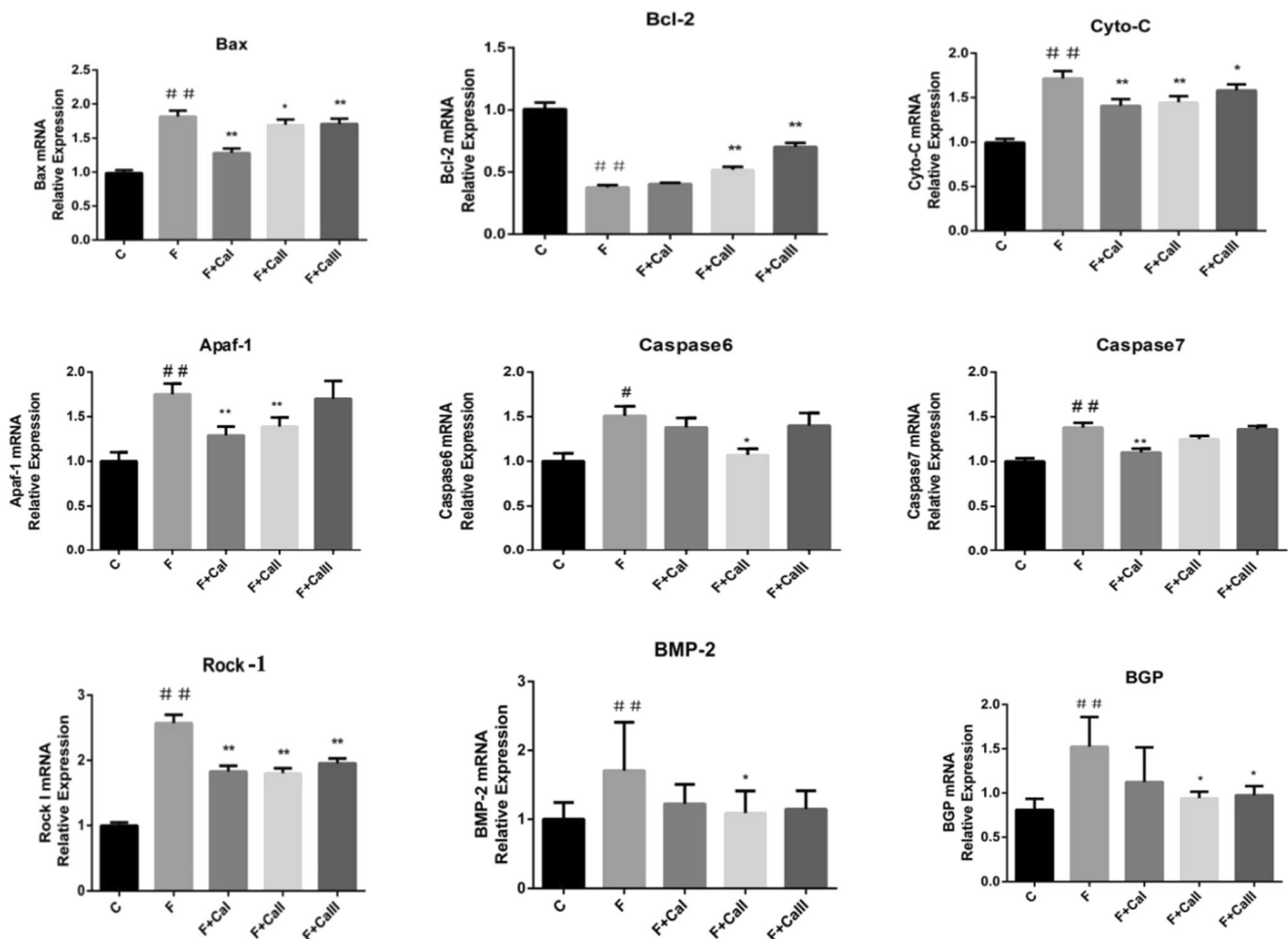
Fig. 4 Effect of Ca on the mRNA expression of osteocyte-associated apoptosis gene in the mitochondrial apoptotic pathway and Rho/ROCK signaling pathway in rat femur subjected to 150 mg/L NaF at the 16th week. $^{\#}P < 0.05$, $^{\#\#}P < 0.01$ as compared with the C group; $^{*}P < 0.05$, $^{**}P < 0.01$ as compared with the F group

with the previous study [28]. Meanwhile, in our previous discussion, we have found that 9 mg/L NaF not only inhibited the proliferation of OB isolated from neonatal rabbit calvarias but also increased intracellular free Ca^{2+} levels by triggering the endoplasmic reticulum (ER) stress. However, 0.5–1 mmol/L Ca^{2+} dramatically enhanced the proliferation of OB cells, whereas 2–8 mmol/L Ca^{2+} had no clear effect on the damage induced by F in the OB cells, in vitro [30]. Nevertheless, increased levels of ER-released cytoplasmic Ca^{2+} may induce mitochondrial membrane potential changes that lead to Cyto-C release and the formation of Apaf-1 oligomerization, which leads to the activation of caspase-9 and the formation of apoptosis complex [31]. Coincidently, this study have authenticated that the mRNA expression of Bax and the protein expression of Cyto-C were significantly upregulated, whereas Bcl-2 was downregulated in the F group, which further demonstrated that 150 mg/L NaF destroyed the mitochondrial structure by damaging the outer membrane structure of mitochondria; meanwhile, activating the mitochondrial apoptotic

pathway mediated by Cyto-C/Apaf-1 inevitably increased osteocyte apoptosis by stimulating the activation of downstream factors including caspase-6 and caspase-7, ultimately resulting in changes in bone metabolism. Surprisingly, 1% Ca supplementation reduced the degree of injured mitochondria by protecting the integrality of mitochondria membrane. In this study, the supplementation of 1% Ca reversed the effect of F on the damaged mitochondrial structure, showing a relatively intact membrane structure and substantial contents with clearly arranged cristae. Thoroughly, we have detected that the increased mRNA expression of mitochondrial apoptotic pathway genes, including Bax, Cyto-C, Apaf-1, and caspase-6 were induced by 150 mg/L NaF exposure, and this pathway were blocked by 1% Ca supplementation in the diet. Nevertheless, this study has found that 150 mg/L NaF inhibited the mRNA expression of Bcl-2, which was consistent with the previous study [25], whereas Ca supplementation increased Bcl-2 expression in bone tissue of fluorosis rats which further demonstrated that Ca inhibited the stimulation
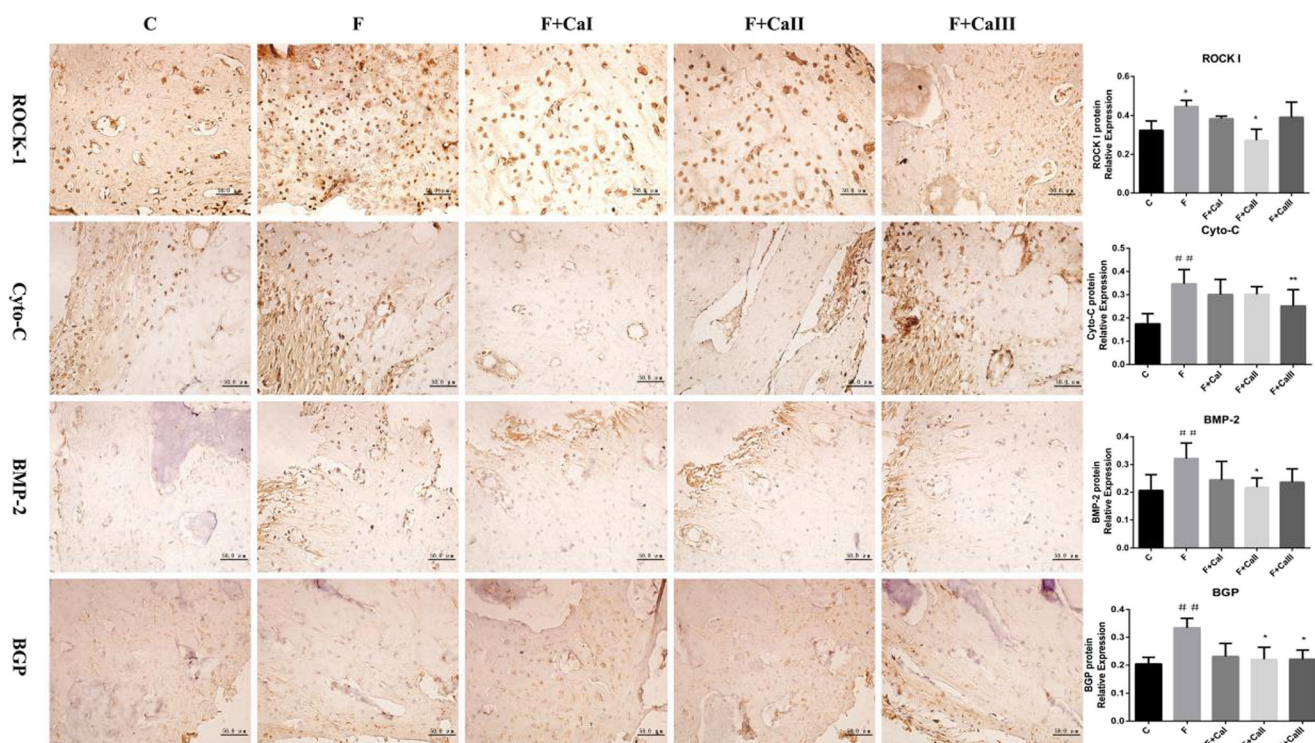
Fig. 5 Immunohistochemical assays to detect the different Ca levels on bone metabolism and mitochondrial pathway as well as Rho/ROCK signaling pathway–related proteins in rat femur after treatment with 150 mg/L NaF at the 16th week (*n* = 8). The graphical representation of immunohistochemistry results of ROCK-1 (bar = 50 μm), Cyto-C (bar = 50 μm), BMP-2 (bar = 50 μm), BGP (bar = 50 μm). #*P* < 0.05, ##*P* < 0.01 as compared with the C group; *#*P* < 0.05, ***P* < 0.01 as compared with the F group

of the mitochondrial apoptosis pathway by increasing the expression of anti-apoptotic genes, thus protecting the complete structure of mitochondria.

ROCK-1, also known as small G protein Rho-associated kinases, was considered as the most central member of the Rho/ROCK signaling pathway [32]. In this study, we have demonstrated that 150 mg/L NaF markedly enhanced the mRNA and protein expression of ROCK-1 in the rat femora. For the first time, our research has shown that Rho/ROCK is involved in the apoptosis of the osteocytes induced by NaF. This might help elucidate the development and therapeutic goals of novel biomarkers for skeletal fluorosis diagnosis. Besides, the mRNA and protein expression of ROCK-1 were markedly reduced with 1% Ca treatment. Previous study has shown that the ROCK-1 molecule is involved in the regulation of mitochondrial fission through the Drp1 protein [33], and specific knockdown of ROCK-1 molecules decreased mitochondrial abnormal division and decreased apoptosis rate in podocytes [34], which was consistent with the present study. There was a study that showed that excessive F-induced abnormal mitochondrial fission is manifested by increases in the number of mitochondria and structural damage to this organelle, by activating the Drp1/Mff signaling pathway, eventually causing the release of Cyto-C and activation of caspase protein family [35]. Thus, F may increase the expression of ROCK-1, which acts on the Drp1/Mff signaling pathway,

inducing mitochondria structural damage and the bone tissue apoptosis.

To predict the development of skeletal fluorosis in advance in clinical practice, plasma Ca, AKP, and StrACP contents were determined. Besides, BMP-2 and BGP are related indices of bone metabolism, which can reflect the degree of bone metabolism activity to some extent [36]. In this study, F treatment decreased the serum Ca content, whereas 2% Ca upregulated it at 12 and 16 weeks (*P* < 0.05), which indicated that the Ca supplementation in the diet restored the blood Ca of the rats with fluorosis, thus decreasing the damage of F to the body. In this experiment, the serum AKP activity of each group of rats decreased in the later stage of the experiment, which may be due to the maturation of experimental animals, the slow growth, and the slow bone turnover. Moreover, this study suggested that F significantly enhanced the StrACP activity, whereas 2% Ca reversed the effect at the 4th week (*P* < 0.05). This indicated that F increased osteoclast StrACP activity and activated osteolytic phenomena, which is consistent with previous research reports [25, 30]. However, the StrACP activity was significantly lower along with the 4th week of 2% Ca supplementation, indicating that Ca could effectively inhibit the activation of osteoclasts induced by F and make osteoclasts activity normal. Normally, BMP-2 is mainly located in bone collagen fibers, periosteum, and bone marrow matrix. However, the increase of BMP-2 number and

activity was mainly attributed to necrosis, absorption, the release of Ca, and secretion of mesenchymal cells [37]. In this study, F significantly increased the protein expression by 26.21% of BMP-2 ($P < 0.01$), showing that F enhanced osteogenesis, which was consistent with previous research reports. Interestingly, 1% Ca reduced the protein expression by 16.15% of BMP-2, indicating that 1% Ca effectively blocked the osteogenesis induced by F. Similarly, the production of BGP increased with the progression of mineralization and OB differentiation. Currently, the protein expression of BGP was markedly augmented in the F group by 28.43%; nevertheless, after the 1% Ca treatment, the protein expression of BGP was decreased by 15.65%.

In summary, this study demonstrated that 150 mg/L NaF induced apoptosis through the Rho/ROCK signaling pathway and mitochondrial apoptosis pathway mediated by Cyto-C/Apaf-1 in the osteocytes, and also destroyed the mitochondrial membrane structure and integrity, further leading to the abnormal bone metabolism. Nevertheless, 1% Ca depressed the mitochondrial apoptosis pathway by increasing the anti-apoptotic gene Bcl-2 expression, and effectively inhibited the hyper-activation of ROCK-1, and it dually protected the structural integrity of the mitochondrial outer membrane and maintained normal cellular metabolic function.

Compliance with Ethical Standards

Conflict of Interest The authors declare that they have no conflict of interest.

References

1. Shruthi MN, Anil NS (2018) A comparative study of dental fluorosis and non-skeletal manifestations of fluorosis in areas with different water fluoride concentrations in rural Kolar. J Family Med Prim Care 7(6):1222–1228. https://doi.org/10.4103/jfmpc.jfmpc_72_18

2. Srivastava RN, Gill DS, Moudgil A, Menon RK, Thomas M, Dandona P (1989) Normal ionized calcium, parathyroid hypersecretion, and elevated osteocalcin in a family with fluorosis. Metab Clin Exp 38(2):120–124. https://doi.org/10.1016/0026-0495(89)90250-3

3. Junrui P, Bingyun L, Yanhui G, Xu J, Darko GM, Dianjun S (2016) Relationship between fluoride exposure and osteoclast markers during RANKL-induced osteoclast differentiation. Environ Toxicol Pharmacol 46:241–245. https://doi.org/10.1016/j.etap.2016.08.001

4. Caetano-Lopes J, Canhão H, Fonseca JE (2007) Osteoblasts and bone formation. Acta Reumatol Port 32(2):103–110

5. Lim E-K, Keem JO, H-s Y, Jung J, Chung BH (2015) Smart nanoprobes for the detection of alkaline phosphatase activity during osteoblast differentiation. Chem Commun (Camb) 51(15):3270–3272. https://doi.org/10.1039/c4cc09620g

6. Wang J, Yang J, Cheng X, Yin F, Zhao Y, Zhu Y, Yan Z, Khodaei F, Ommati MM, Manthari RK, Wang J (2019) Influence of calcium supplementation against fluoride-mediated osteoblast impairment in vitro: involvement of the canonical Wnt/β-catenin signaling pathway. J Agric Food Chem 67(37):10285–10295. https://doi.org/10.1021/acs.jafc.9b03835

7. Ducheyne P, el-Ghannam A, Shapiro I (1994) Effect of bioactive glass templates on osteoblast proliferation and in vitro synthesis of bone-like tissue. J Cell Biochem 56(2):162–167. https://doi.org/10.1002/jcb.240560207

8. Kylmaoja E, Nakamura M, Tuukkanen J (2016) Osteoclasts and remodeling based bone formation. Curr Stem Cell Res Ther 11(8):626–633. https://doi.org/10.2174/1574888x10666151019115724

9. Hayman AR (2008) Tartrate-resistant acid phosphatase (TRAP) and the osteoclast/immune cell dichotomy. Autoimmunity 41(3):218–223. https://doi.org/10.1080/08916930701694667

10. Reddy GS, Rao BS (1971) Effect of dietary calcium, vitamin C and protein in development of experimental skeletal fluorosis. II. Calcium turnover with 45Ca; calcium and phosphorus balances. Metab Clin Exp 20(7):650–656. https://doi.org/10.1016/0026-0495(71)90078-3

11. Sun F, Li X, Yang C, Lv P, Li G, Xu H (2014) A role for PERK in the mechanism underlying fluoride-induced bone turnover. Toxicology 325:52–66. https://doi.org/10.1016/j.tox.2014.07.006

12. Eguchi K, Akiba Y, Akiba N, Nagasawa M, Cooper LF, Uoshima K (2018) Insulin-like growth factor binding protein-3 suppresses osteoblast differentiation via bone morphogenetic protein-2. Biochem Biophys Res Commun 507(1–4):465–470. https://doi.org/10.1016/j.bbrc.2018.11.065

13. Huo L, Liu K, Pei J, Yang Y, Ye Y, Liu Y, Sun J, Han H, Xu W, Gao Y (2013) Fluoride promotes viability and differentiation of osteoblast-like Saos-2 cells via BMP/Smads signaling pathway. Biol Trace Elem Res 155(1):142–149. https://doi.org/10.1007/s12011-013-9770-0

14. Yan X, Hao X, Nie Q, Feng C, Wang H, Sun Z, Niu R, Wang J (2015) Effects of fluoride on the ultrastructure and expression of type I collagen in rat hard tissue. Chemosphere 128:36–41. https://doi.org/10.1016/j.chemosphere.2014.12.090

15. Estaquier J, Vallette F, Vayssiere J-L, Mignotte B (2012) The mitochondrial pathways of apoptosis. Adv Exp Med Biol 942:157–183. https://doi.org/10.1007/978-94-007-2869-1_7

16. Jeng PS, Inoue-Yamauchi A, Hsieh JJ, Cheng EH (2018) BH3-dependent and independent activation of BAX and BAK in mitochondrial apoptosis. Curr Opin Physiol 3:71–81. https://doi.org/10.1016/j.cophys.2018.03.005

17. Singh BK, Tripathi M, Chaudhari BP, Pandey PK, Kakkar P (2012) Natural terpenes prevent mitochondrial dysfunction, oxidative stress and release of apoptotic proteins during nimesulide-hepatotoxicity in rats. PLoS One 7(4):e34200–e34200. https://doi.org/10.1371/journal.pone.0034200

18. Chauhan D, Hideshima T, Rosen S, Reed JC, Kharbanda S, Anderson KC (2001) Apaf-1/cytochrome c-independent and Smac-dependent induction of apoptosis in multiple myeloma (MM) cells. J Biol Chem 276(27):24453–24456. https://doi.org/10.1074/jbc.C100074200

19. Farmer T, O'Neill KL, Naslavsky N, Luo X, Caplan S (2019) Retromer facilitates the localization of Bcl-xL to the mitochondrial outer membrane. Mol Biol Cell 30(10):1138–1146. https://doi.org/10.1091/mbc.E19-01-0044

20. Vishnubhotla R, Bharadwaj S, Sun S, Metlushko V, Glover SC (2012) Treatment with Y-27632, a ROCK inhibitor, increases the proinvasive nature of SW620 cells on 3D collagen type 1 matrix. Int J Cell Biol 2012:259142–259142. https://doi.org/10.1155/2012/259142

21. Bharadwaj S, Thanawala R, Bon G, Falcioni R, Prasad GL (2005) Resensitization of breast cancer cells to anoikis by tropomyosin-1:

role of Rho kinase-dependent cytoskeleton and adhesion. Oncogene 24(56):8291–8303. https://doi.org/10.1038/sj.onc.1208993

22. Nóbrega DF, Leitão TJ, Cury JA, Tenuta LMA (2019) Fluoride binding to dental biofilm bacteria: synergistic effect with calcium questioned. Caries Res 53(1):10–15. https://doi.org/10.1159/000488598

23. Everts V, Niehof A, Tigchelaar-Gutter W, Beertsen W (2019) Transmission electron microscopy of bone. Methods Mol Biol (Clifton, NJ) 1914:617–629. https://doi.org/10.1007/978-1-4939-8997-3_32

24. Malin AJ, Riddell J, McCague H, Till C (2018) Fluoride exposure and thyroid function among adults living in Canada: effect modification by iodine status. Environ Int 121(Pt 1):667–674. https://doi.org/10.1016/j.envint.2018.09.026

25. Wang J, Yang J, Cheng X, Xiao R, Zhao Y, Xu H, Zhu Y, Yan Z, Ommati MM, Manthari RK, Wang J (2019) Calcium alleviates fluoride-induced bone damage by inhibiting endoplasmic reticulum stress and mitochondrial dysfunction. J Agric Food Chem 67(39):10832–10843. https://doi.org/10.1021/acs.jafc.9b04295

26. Hou T, Kolba N, Glahn RP, Tako E (2017) Intra-amniotic administration (Gallus gallus) of Cicer arietinum and Lens culinaris prebiotics extracts and duck egg white peptides affects calcium status and intestinal functionality. Nutrients 9(7):785. https://doi.org/10.3390/nu9070785

27. Carvalho TS, Bönecker M, Altenburger MJ, Buzalaf MAR, Sampaio FC, Lussi A (2015) Fluoride varnishes containing calcium glycerophosphate: fluoride uptake and the effect on in vitro enamel erosion. Clin Oral Investig 19(6):1429–1436. https://doi.org/10.1007/s00784-014-1363-6

28. Wei Q, Luo Q, Liu H, Chen L, Cui H, Fang J, Zuo Z, Deng J, Li Y, Wang X, Zhao L (2018) The mitochondrial pathway is involved in sodium fluoride (NaF)-induced renal apoptosis in mice. Toxicol Res (Camb) 7(5):792–808. https://doi.org/10.1039/c8tx00130h

29. Aurélien O, Laurent B, Nicole G, Emmanuelle G, Annie V, Pascale B, Guy L (2003) Loss of OPA1 perturbates the mitochondrial inner membrane structure and integrity, leading to cytochrome c release and apoptosis. J Biol Chem 278(10):7743–7746. https://doi.org/10.1074/jbc.C200677200

30. Wang J, Zhao Y, Cheng X, Li Y, Xu H, Manthari RK, Wang J (2018) Effects of different Ca(2+) level on fluoride-induced apoptosis pathway of endoplasmic reticulum in the rabbit osteoblast in vitro. Food Chem Toxicol 116(Pt B):189–195. https://doi.org/10.1016/j.fct.2018.04.013

31. Ben-Hail D, Shoshan-Barmatz V (2016) VDAC1-interacting anion transport inhibitors inhibit VDAC1 oligomerization and apoptosis. Biochim Biophys Acta 1863(7 Pt A):1612–1623. https://doi.org/10.1016/j.bbamcr.2016.04.002

32. Zhang WM, Cao P, Xin L, Zhang Y, Liu Z, Yao N, Ma YY (2019) Effect of miR-133 on apoptosis of trophoblasts in human placenta tissues via Rho/ROCK signaling pathway. Eur Rev Med Pharmacol Sci 23(24):10600–10608. https://doi.org/10.26355/eurrev_201912_19755

33. Collins SJ, Tumpach C, Groveman BR, Drew SC, Haigh CL (2018) Prion protein cleavage fragments regulate adult neural stem cell quiescence through redox modulation of mitochondrial fission and SOD2 expression. Cell Mol Life Sci 75(17):3231–3249. https://doi.org/10.1007/s00018-018-2790-3

34. Ayanga BA, Badal SS, Wang Y, Galvan DL, Chang BH, Schumacker PT, Danesh FR (2016) Dynamin-related protein 1 deficiency improves mitochondrial fitness and protects against progression of diabetic nephropathy. J Am Soc Nephrol 27(9):2733–2747. https://doi.org/10.1681/ASN.2015101096

35. Zhou BH, Wei SS, Jia LS, Zhang Y, Miao CY, Wang HW (2020) Drp1/Mff signaling pathway is involved in fluoride-induced abnormal fission of hepatocyte mitochondria in mice. Sci Total Environ 725:138192. https://doi.org/10.1016/j.scitotenv.2020.138192

36. Yang B, Lin X, Tan J, She X, Liu Y, Kuang H (2016) Root bark of Sambucus williamsii Hance promotes rat femoral fracture healing by the BMP-2/Runx2 signaling pathway. J Ethnopharmacol 191:107–114. https://doi.org/10.1016/j.jep.2016.05.017

37. Nakamura Y, Wakitani S, Nakayama J, Wakabayashi S, Horiuchi H, Takaoka K (2003) Temporal and spatial expression profiles of BMP receptors and noggin during BMP-2-induced ectopic bone formation. J Bone Miner Res 18(10):1854–1862. https://doi.org/10.1359/jbmr.2003.18.10.1854